CORRECTION OF THE ABOVE WATER RADIOMETRIC MEASUREMENTS FOR THE SKY DOME REFLECTION, ACCOUNTING FOR POLARIZATION

***Richard Santer*[1,5], *Francis Zagolski*[1,2], *Kathryn Barker*[3], *and Jean-Paul Huot*[4]**

[1] *ADRINORD, 2 rue des Canonniers, F59000, Lille E-mail: santer.richard@yahoo.fr*

[2] *PARBLEU Ltd Technologies Inc., 79 Veilleux street, St Jean-sur-Richelieu (QC), J3B-3W7 – CANADA.E-mail: Francis_Zagolski@yahoo.ca*

[3] *ARGANS Ltd, Unit 3 Drake Building, Tamar Science Park, 15 Davy Road, Derriford, Plymouth, PL6-8BY – UK, E-mail: KBarker@argans.co.uk*

[4] *ESA Space Environment and Effects Section(TEC-EES), Keplerlaan 1, Noordwijk, 2200AG – THE NETHERLANDS E-mail: Jean-Paul.Huot@esa.int*[1]

[5] *ULCO, MREN, 32 avenue Foch, F62930Wimereux, E-mail: santer@univ-littoral.fr*

ABSTRACT

The water-leaving radiance measurement is a key element in the validation of atmospheric corrections over ocean. The latter requires the correction for the *Fresnel* reflection of the sky dome by the water surface. Currently, this correction is achieved with a measurement of the sky radiance and the use of a *Fresnel* reflection coefficient, ignoring the polarisation processes. Our objective is to illustrate the bias induced by neglecting the polarisation in the reflected sky dome by the sea surface. Results from this study clearly stress that the polarization has to be accounted for.

1 INTRODUCTION

A standard sky dome correction is employed for removing the *Fresnel* reflection contribution from the upwelling radiance, $L^{\uparrow}$, measured by the field sensor to get the water-leaving radiance:

$$L_w^{\uparrow} = L^{\uparrow} - R(\theta_v, w_s)\cdot L^{\downarrow} - L_G(w_s)\cdot\exp(-\tau/\mu_s) \quad (1)$$

where $L^{\downarrow}$ is the downwelling atmospheric radiance collected at sea level. Both $L^{\uparrow}$ and $L^{\downarrow}$ are acquired with the same view azimuth angle, VAA (ϕ_v), but with two opposite values of the view zenith angle view zenith angle, VZA (θ_v).

L_G represents the Sun glint contribution at bottom of the atmosphere (BOA). L_G is attenuated on the direct path. This correction is marginal for most of the geometrical conditions.

The *Fresnel* reflection coefficient (R) depends on the wind-speed w_s, the driving parameter for the roughness of the sea surface. Tab. 1 gives R for a VZA=40°. at 3 w_s following [1, 2]

Table 1: Reflection coefficient (in percent) versus the wind speed

w_s(m/s)	1.5	5	10
R_1	2.63	2.84	3.29

The standard correction of sky dome reflection ignores the polarization processes. Indeed, when VZA is large enough, the *Fresnel* reflection becomes polarized. Fig. 1 gives the three components of the Fresnel matrix defines as: defined as:

$$R = \begin{pmatrix} R_1 & R_2 & 0 \\ R_2 & R_1 & 0 \\ 0 & 0 & R_3 \end{pmatrix} \text{ with } \begin{cases} R_1 = (r_{//}^2 + r_{\perp}^2)/2 \\ R_2 = (r_{//}^2 - r_{\perp}^2)/2 \\ R_3 = r_{//}\cdot r_{\perp} \end{cases} \quad (2)$$

The Fresnel coefficients are plotted in Fig. 1. The *Fresnel* reflection of incident sky light on a flat sea surface is fully polarized at the *Brewster*'s angle ($\theta_B \approx 53°$) which corresponds to the extinction of electric field polarized in the reflection plane ($r_{//}=0$). At this *Brewster*'s angle, the two first terms of the Fresnel matrix, R_1 and R_2, are equal and opposite.

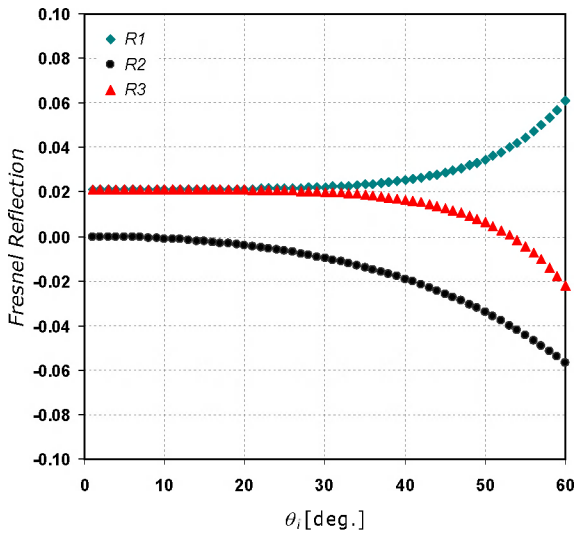

Figure 1: Angular variation of Fresnel reflection terms (R_1, R_2, R_3). θ_i is the zenith angle of the incident light beam on the flat «air-water» interface (n_w=1.34).

Because the sky radiance is also polarised, then these two combined effects bias Eq. 1. Let's take an extreme case which corresponds to a sun in our back when taking measurements at $\theta_v \approx 53°$. The SZA is 37° and we have a pure molecular atmosphere. The scattering angle is 90°. and the Rayleigh polarisation ratio is 100 percent. In that case, the direction of polarisation is perpendicular to the principal plane (which is also the reflection plane if the sea surface is a mirror). The Stokes parameters describing the down-welling radiance are in this case:

$$L^{\downarrow} = Q^{\downarrow} \text{ and } U^{\downarrow} = V^{\downarrow} = 0 \qquad (3)$$

The standard correction assumed that:

$$L^{\uparrow} = R_1 \, L^{\downarrow} \qquad (4)$$

Actualy, according to Eq. (2),we have:

$$L^{\uparrow} = R_1 \, L^{\downarrow} + R_2 \, Q^{\downarrow} \qquad (5)$$

and in this case:

$$L^{\uparrow} = 2R_1 \, L^{\downarrow} \qquad (6)$$

The standard procedure omits a factor 2.

Of course, it is an extreme case for which we can conduct a simple computation. But it illustrates the problem on an academic way.
The general problem is also more complex than what we just explain for an observation in the principal plane. In that plane, the direction of polarisation, both for the atmospheric scattering and for the Fresnel reflection, is perpendicular to the principal plane. Because Eq. (4) is arithmetic the introduction of the polarisation increases the sky dome reflection. However, depending on the geometry and particularly on the direction of the atmospheric polarisation relative to the plane of reflection, the polarisation may decrease the correction.

We have an analogy with the pure Rayleigh scattering. Accounting for the polarisation results in some geometry of a positive bias on the atmospheric radiance and in some others of a negative bias. In average values, such as the spherical albedo, a scalar code gives the same result than a vector code which includes the polarisation.

2 A SYNTHETIC DATA BASE IN POLARISATION

By definition, the computation (or measurement) of $L^{\uparrow}$ requires first to know the Stokes parameters of the down-welling radiance field. Second, we have to apply the Fresnel matrix. It is a classical problem in radiative transfer. The vector version of the successive orders of scattering code (SO) was used for computing the radiative transfer within a coupled *«Ocean-Atmosphere»* system [3]. A simulator was realized [4] to output in the MERIS spectral bands the BOA down-welling and upwelling radiance fields (L, Q, U). The viewing geometry (θ_v=40°., ϕ_v=135 °.) is as recommended in [2]. The reflection coefficient is simply defined by:

$$R_{boa} = L^{\uparrow} / L^{\downarrow} \qquad (7)$$

We compute here $L^{\uparrow}$ accounting for the polarisation both for the atmospheric scattering and for the *Fresnel* reflection above a dark ocean. We use a standard molecular atmosphere, a set of 4 aerosol models (*M1*, *M2*, *M3*, *M4*) which are 4 -power law size distributions associated with 4 Angstroem exponents (α = -0.3, -0.9, -1.5, -1.9) and non-absorbing particles with a refractive index (m) of 1.44 and a set of 4 aerosol optical thicknesses (AOT560) at 560 *nm*: 0 (Rayleigh), 0.3, 0.6 and 0.9.

Fig. 2 gives the phase functions for the Rayleigh and for the aerosol models versus the SZA with an increase in forward scattering. The phase function and the polarisation ratio do not depend on the wavelength for the Rayleigh but also for the aerosols because of the selection of a power law for the size distribution.

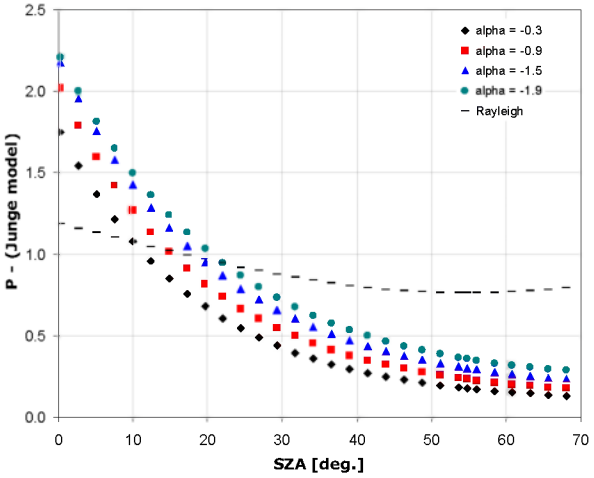

Figure 2: Phase function p as function of SZA in the defined viewing geometry for molecules and 4 Junge models (α=-0.3, -0.9, -1.5, 1-.9).

For the polarisation ratio, Fig. 3, the Rayleigh maximum is located in the SZA range *50* ° to *60* °. which is a usual value for measurements at mid latitude around 10 pm. The aerosols also polarise with a maximum which is a little shifted towards larger SZA angles. The polarisation by the aerosols increases when they become smaller, when α decreases.

From the inherent optical properties to the apparent ones, the Rayleigh reflectance is in λ^{-4} and does not

vary much versus the SZA (same air mass for a flat phase function). At a given wavelength, the aerosol reflectance decreases with the SZA. The multiple scatterings depolarised. Therefore, for the Rayleigh, the influence of the polarization on R is less effective in the blue compared to the red. This depolarisation effect also applies to the aerosols but more effectively to be linked to a smaller spectral dependence of the AOT.

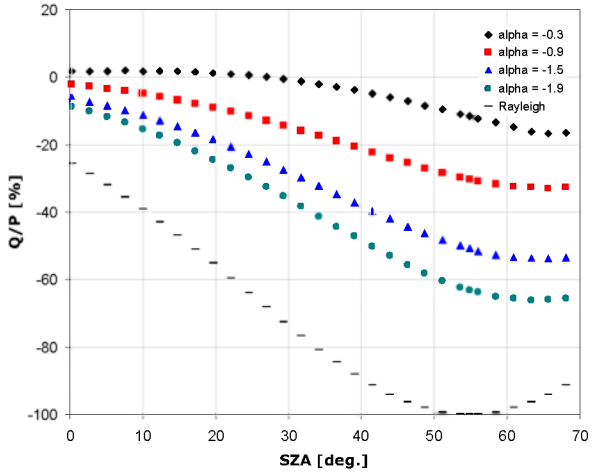

Figure 3: Same as figure 2 but for the polarisation ratio.

We describe the surface roughness with the Cox-Munk wave slope distribution [5] and a set of 3 wind-speeds (1.5, 5.0 and 10 *m/s*). The ocean is black.

The SO code also returns the direct and total T (direct + diffuse) down-welling atmospheric transmittances. The direct is for the sun-glint correction. The total is used to convert radiance into reflectance as:

$$\rho = \frac{\pi L^{\uparrow}}{E_s(\mu_s)} = \frac{L^{\uparrow}}{\mu_s T(\mu_s)} \qquad (8)$$

The extraterrestrial spectral solar irradiance in the SO code is π which gives the right part of Eq. (7).

3 INFLUENCE OF THE POLARISATION

3.1 On the reflection coefficient

Fig. 4 gives the reflection coefficient at one wavelength for one aerosol model at a given wind speed. The dependence on the SZA corresponds to the dependence of the polarised radiance: the polarisation ratio, P, is maximum at a scattering angle of 90° which corresponds here to SZA to about *50 °*. Eq. (5) invokes $Q^{\downarrow}$ not $P^{\downarrow}$ but the product of $P^{\downarrow}$ by $L^{\downarrow}$. Therefore, because $L^{\downarrow}$ increases in forward scattering, the maximum of R_{boa} is shifted towards a smaller scattering angle.

The maximum of R_{boa} corresponds to the Rayleigh case which is the main source of polarisation. The influence of the aerosols is to depolarise the Rayleigh scattering. According to table 1, R=*2.63* and we are always above this value. In the considered geometry, the direction of polarisation is always perpendicular to the plane of reflection. Therefore, $R_2\ Q^{\downarrow}$ is positive.

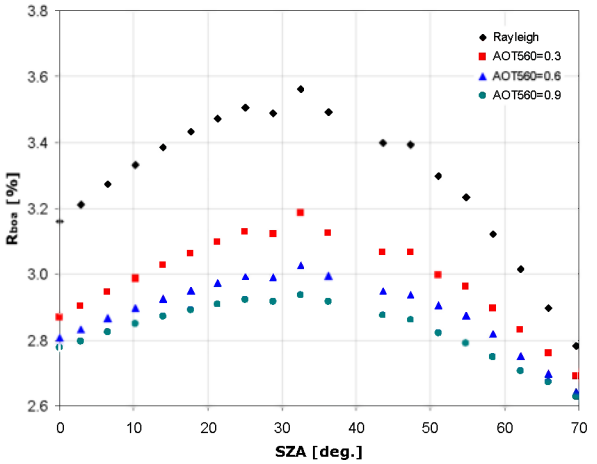

Figure 4: Fresnel reflection coefficient (R_{boa}) at 510 nm as function of SZA, derived from the SO computations over wind-roughened black sea surfaces, (1.5 m/s) under 4 atmospheres: AOT560=0, 0.3, 0.6 and 0.9 for the 3rd Junge model (α=-1.5).

Fig. 5 illustrates the dependence of R_{boa} with the wind speed. The effect is well known and was already account for in the scalar approach as reflected in Tab. 1. It corresponds to the weight of the Fresnel coefficients by the wave slope distribution function, which is quite symmetrical. The Fresnel coefficients, around a VZA of *40 °*, increase with the incident angle. Therefore, we have this increase of R_{boa}, which is more pronounced when the polarisation is accounted for.

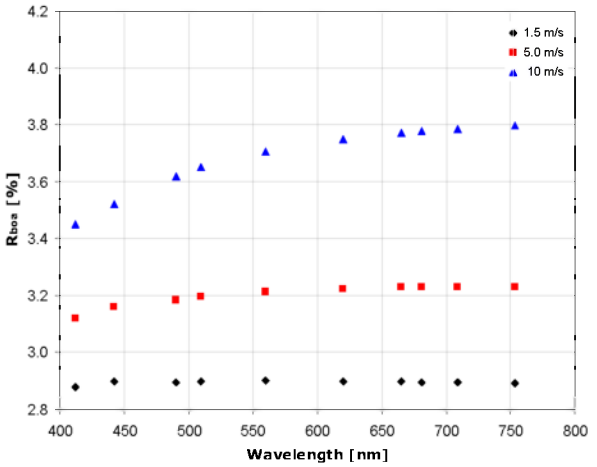

Figure 5: Spectral dependence of the Fresnel reflection coefficient (R_{boa}) for 3 wind-speeds (1.5, 5 and 10 m/s. The computations are for SZA=58 ° and with an

aerosol layer characterized by the 3rd aerosol model (α=-1.5) and an AOT560 of 0.3.

At a given wind speed, Fig. 5also gives the spectral dependence of R_{boa}. R_{boa} slightly decreases towards the blue mainly at larger wind speeds. The scattering angle is *90* °, the maximum of the Rayleigh polarisation, at least for the specular reflection. When the roughness of the sea increases, we leave this maximum. For the aerosols, the maximum of polarisation is *100* °, which counterbalances the wind effect on the Rayleigh mostly towards the red.

We expect to see the impact of the aerosol model mostly in the red. Fig.6 reports R at 753 nm for an *AOT560=0.3*. We see some computation artefacts around 40° corresponding to a bad restitution of the aerosol phase function in Fourier series at VZA=SZA which occurs mainly for large particles. It is the case with mainly with M1. At the maximum of R, we see an extreme difference of 0. 4 which is more effective than the wind effect as reported in Tab. 1.

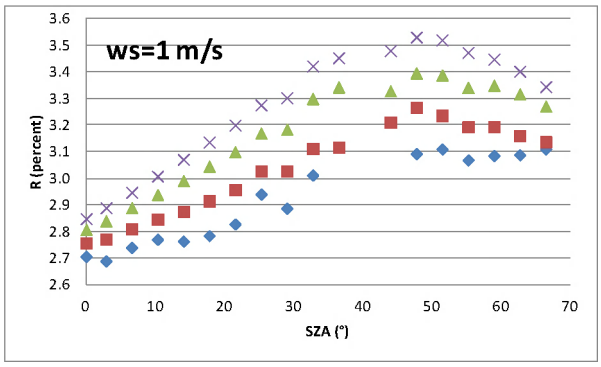

Figure 6: Reflection coefficient at 753 nm versus the SZA. Computations have been completed for 4 aerosol models: M1 (diamond), M2 (square), M3 (triangle) and M4 (cross) for a wind speed of 1 m/s.

3.2 On the water reflectance

The specular case

Let's start by the specular reflection. By using Eqs. 2 and 8, the bias on the reflected sky radiance ($d\rho_{sky}$) when neglecting polarization can then be estimated as:

$$d\rho_{sky} = \frac{R_2 Q^{\uparrow}}{\mu_s \cdot T(\theta_s)} \qquad (9)$$

This absolute biais is also the absolute bias on the water - reflectance as reported in Fig. 7. The sky dome corrrection in this geometry is positive. Therefore, after correction, the water reflectance becomes lower. First of all the behavior in VZA of $d\rho_{wy}$ does not fully follows the the behavior of R. The main effect comes from the denominator of Eq. (9) with it decrease when SZA increases. At 442 nm, the Rayleigh scattering dominates and the influence of the aerosols is a second order effect. Conversely at 753 nm, the influence of the aerosols appears. The aerosol model corresponds to an α value which occurs more frequenly in coastal waters.

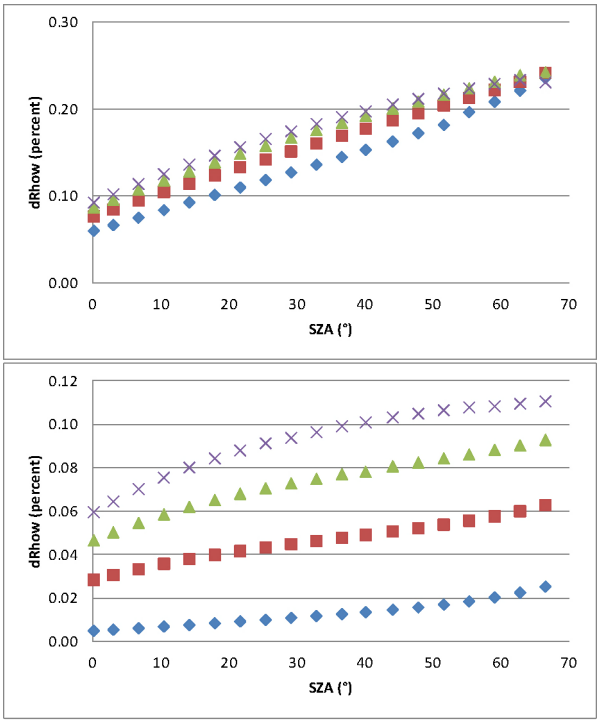

Figure 7: Bias on the water reflectance induced by a standard protocol ignoring polarisation. Computations have been completed at 442.5 nm (above) and 753.75 nm (below) for 4 atmospheres: AOT560=0(diamond), 0.3(square), 0.6(triangle) and 0.9(cross) for the 3rd model (α=-1.5).

Fig. 8 uses the same computation but to study the spectral dependence. As expected the bias decreases with wavelength simply because the atmospheric radiance decreases with it. This bias appears substantial bearing in mind that the value of the water reflectance in this spectral domain is only of few percent.

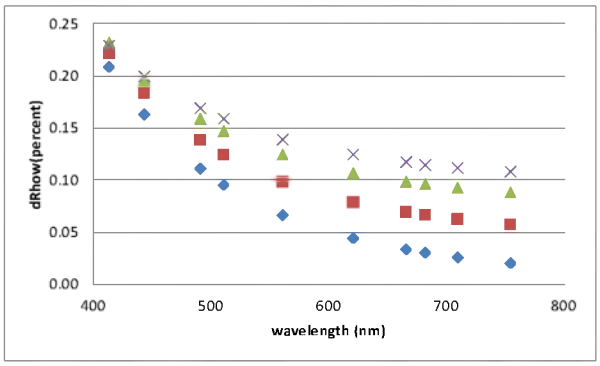

Figure 8: Same as Fig. 6 but versus the wavelength for a SZA=59 °.

Influence of the wind speed

The bias on the reflected sky radiance ($d\rho_{sky}$) corresponds to the use of a new reflection coefficient R_{boa} compared to the old one R_1 as reported in Tab. 1 which are both applies to the down-welling atmospheric radiance $L^{\downarrow}$.

$$d\rho_{sky} = \frac{(R_{boa} - R_1)\, L^{\downarrow}}{\mu_s \cdot T(\theta_s)} \qquad (10)$$

$L^{\downarrow}$ and T do not depend much on the surface reflection. Therefore ($d\rho_{sky}$) mainly depends on the difference between the two reflection coefficients which varies with the wind speed.

Fig. 9 reports the results for a wind speed of 1 m/s for an AOT560=0.3 and for the three aerosol models. For model 3, the results are very consistant with the specular case as reported in Fig. 8. Of course it is what we expect but it remains a good opportunity to validate the SO code outputs.

The influence of the aerosol model can also study from Fig. 9. In the blue, the Rayleigh scattering dominates (as it is shown as well in Fig. 8). At a given AOT, the role of the aerosol models appears in the NIR. As already explained in Fig. 3, the smaller they are and the higher they polarised, at least for this geometry. From an oceanic type of aerosols *(α=-0.3)* to small aerosols *(α=- 1-.9)*, the difference is noticeable.

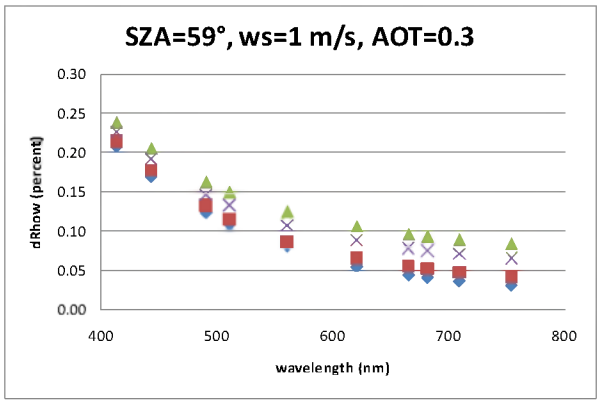

Figure 9: Wind speed of 1 m/s. Absolute bias on the water reflectance versus the wavelength: The AOT at 550 nm is 0.3 for M1 (blue diamond), M2 (red square), M3 (blue cross) and M4 (green triangle)

Fig. 10, in a comparison to Fig. 9, gives the influence of the wind speed. Compare to the scalar case, the effect of the wind speed is emphasised by the polarized component: the angular dependence of R_2 around a VZA of 40° is even more important that the dependence of R_1. We should be able to see something depending on the wind. The correction doubles in all the spectral range from 1 m/s to 10 m/s. In the blue, the correction is in absolute value substantial and important in relative values in the red.

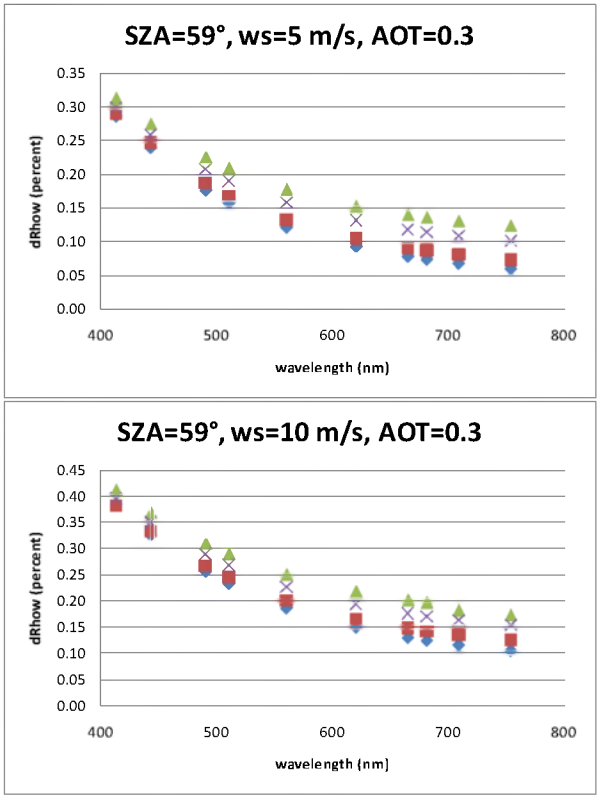

Figure 10: Same as Fig. 8 but with two different wind speeds of 5 m/s and 10 m/s

3.3 The polarisation of the aerosols

Figs. 6, 9 and 10 suggest that the polarization by the aerosols has to be accounted for, mainly for the correction in the NIR. The spectral dependence of the AOT can be directly derived from the measurements of the atmospheric radiance. As a first approximation, we can compute the Angstroem coefficient as:

$$\alpha = Ln((\rho^{\downarrow}(\lambda) - \rho_R^{\downarrow}(\lambda))/\,(\rho^{\downarrow}(\lambda') - \rho_R^{\downarrow}(\lambda'))/\,Ln(\lambda/\lambda') \qquad (11)$$

The atmospheric reflectance $\rho^{\downarrow}(\lambda)$ is corrected from the Rayleigh reflectance $\rho_R^{\downarrow}(\lambda)$ to get the aerosol reflectance. At first order, the ratio of the aerosol reflectance between the two wavelengths at the edges of the spectral domain, is the ratio of the AOT. Alternatively, a spectral linear regression on the aerosol reflectance can be done in log-log to obtain α.

The selection of a power law size distribution associated to α is the easier way to define the aerosol model. The missing parameter is the refractive index. As soon as you have the size distribution and the refractive index, you know the phase function and

therefore, you can derive the AOT from the aerosol reflectance.

Both the 4 power law models employed in the previous sections correspond to the case of aerosols characterized by a non-absorbing refractive index (m) of 1.44. Knowing that the polarization has to be sensitive to m, a study of the influence of the aerosol polarization has been conducted with the same set of power law size distributions, adding two values of refractive index (1.33 and 1.55). The influence of the polarisation of the aerosol is noticeable in the NIR or small aerosols. For the small particles, the Mie theory falls in the Rayleigh-Gans domain for which the polarisation decreases with m.

Fig. 11 reports R for the three refractive indices. The dependence in SZA corresponds to what we presented in Fig. 3. The increase from m=*1.33* to *1.55* is linked to the corresponding increase of the aerosol polarisation and mainly appears in the NIR.

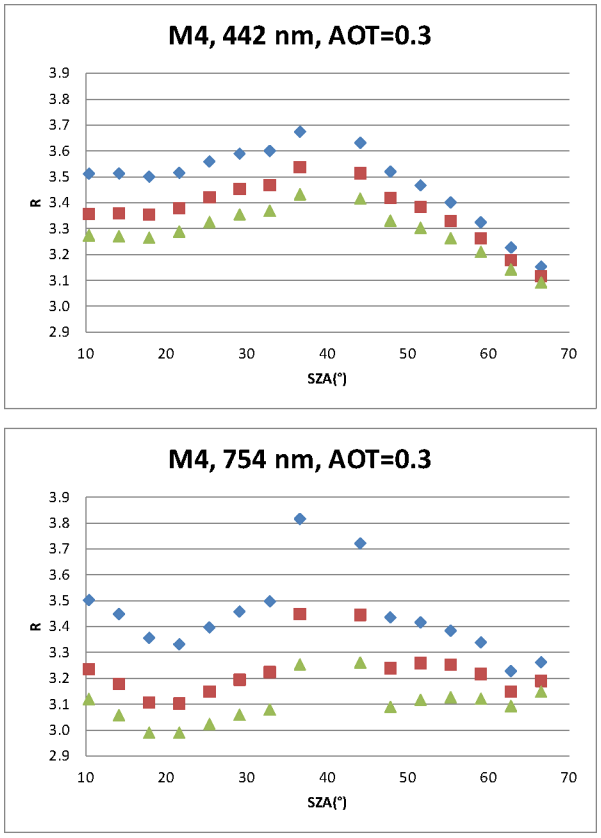

Figure 11: Computation of the reflection coefficient at two wavelengths versus SZA for the aerosol model 4, an AOT560 of 0.3, a wind speed o 1 m/s. The plots correspond to three values of the refractive index: 1.33 (diamond), 1.44(square) and 1.55(triangle)

By using the refractive index of *1.44* as reference, the bias on the sky dome reflection (*i.e.*, the sensitivity of R to the refractive index) can then be computed as:

$$d\rho_{sky} = \frac{(R_m - R_{144})\, L^{\downarrow}_{144}}{\mu_s \cdot T_{144}(\theta_s)}, \qquad (11)$$

in which R_m stands for the *Fresnel* reflection coefficients at the refractive index m (1.33 or 1.55), and $T_{144}(\theta_s)$, L and R_{144} respectively, the total down-welling transmittance, the atmospheric radiance and the *Fresnel* reflection coefficient at the reference value m of 1.44. The results on the bias are reported in Fig. 12. The error is marginal even in the NIR. Therefore the influence of the aerosols can be evaluated through the knowledge of the AOTs.

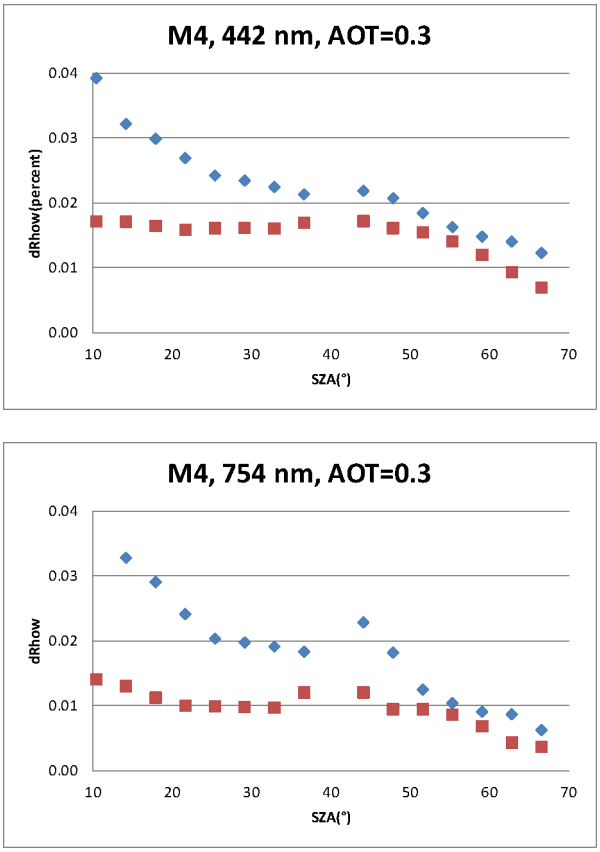

Figure 12: Bias on the water reflectance induced by an error on the aerosol refractive index at two wavelengths versus SZA for the aerosol model 4, an AOT560 of 0.3, a wind speed o 1 m/s. The plots correspond to a difference in refractive index from 1.33 to 1.44(diamond), 1.44 to 1.55 (square).

3.4 Influence of the azimuth

The initial protocol is to measure at *135* ° in azimuth from the sun. Nevertheless some measurements are not acquired in this geometry. It is the case for the SeaPRISM instrument [4] or simply the case from vessel when the cape cannot be maintained.

Fig. 13 computes R first for a pure Rayleigh atmosphere and second for the aerosol model 4, AOT560=0. The wind speed is 7.2 m/s. The direct sun-glint has been corrected. Following [1], $R=3.02$.

We first see that the maximum of R is in the back scattering first because the degree of polarisation is maximum and second because the direction of polarisation is perpendicular to the plane of reflection. The introduction of the aerosols depolarises in the blue. What is true at $180°$ remains valid with a lesser extent at $135°$… However, we really have a different behaviour at 90° mostly at $SZA=60°$. The degree of polarisation becomes substantial but in the same time the direction of polarisation moves to be in the reflection plane. The polarisation in that case reduces the sky reflection.

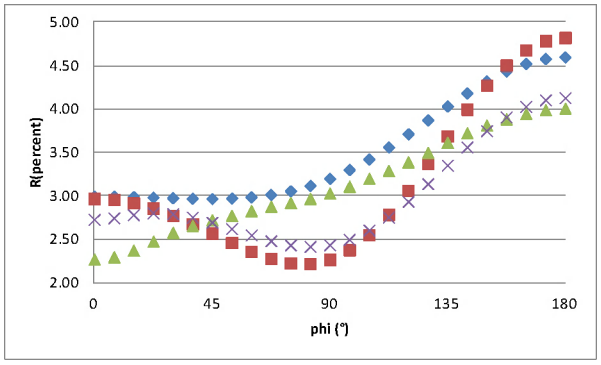

Figure 13: Influence of the azimuth on the reflection coefficient computed at 412 nm for a wind speed of 7.2 m/s. Atmospheric conditions correspond first to a pure molecular atmosphere at SZA=30° (diamond) and 60° (square) and second adding aerosols (M4, AOT560=0.3) at SZA=30° (triangle) and 60° (cross)

The bias in reflectance on the evaluation of the sky dome correction can be first computed for the specular case using Eq. 9 and the polarized radiance Q provided by the SO code. For a roughness sea surface, we use Eq. 11. The results, reported in Fig. 14 and 15, are consistent at $\phi=135^o$. as reported in Fig. 6 to 9. At $\phi=90^o$, for $SZA=29^o$., the effect is small simply because Q is small, combining the degree of polarisation with it direction. At $\phi=90^o$ for $SZA=59^o$., the correction becomes substantial. Conversely to $\phi=135^o$., the new correction of the sky dome reflection at $\phi=90^o$. increases the measurement of the water reflectance. As soon as we introduced the aerosols, we see the reflection of their large forward scattering, including for Q, which provoked a large correction at $SZA=59^o$. and $ws=7.2$ m/s

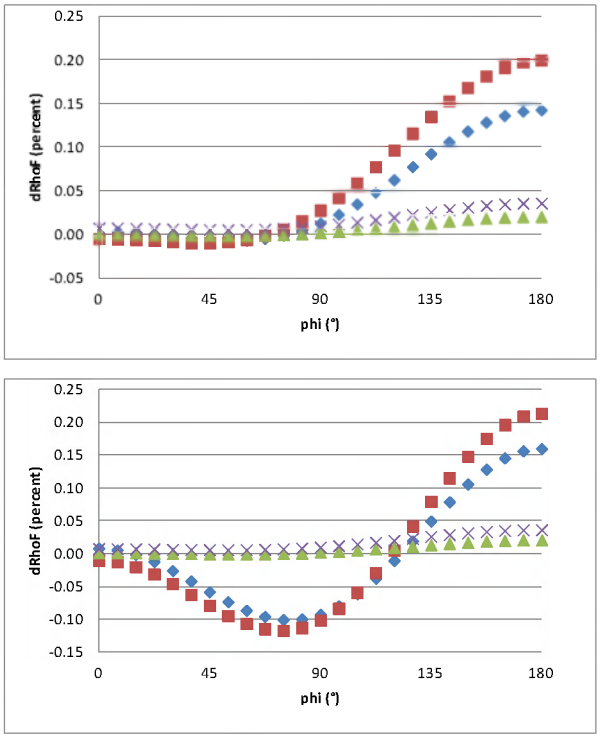

Figure 14: Influence of the azimuth on the bias on the reflected atmospheric reflectance computed for a pure molecular atmosphere at SZA=30°.(above) and 60° .(below).Reflection is specular (diamond at 412 nm and triangle at 665 nm) and for a wind speed of 7.2 m/s (square at 412 nm and cross at 665 nm)

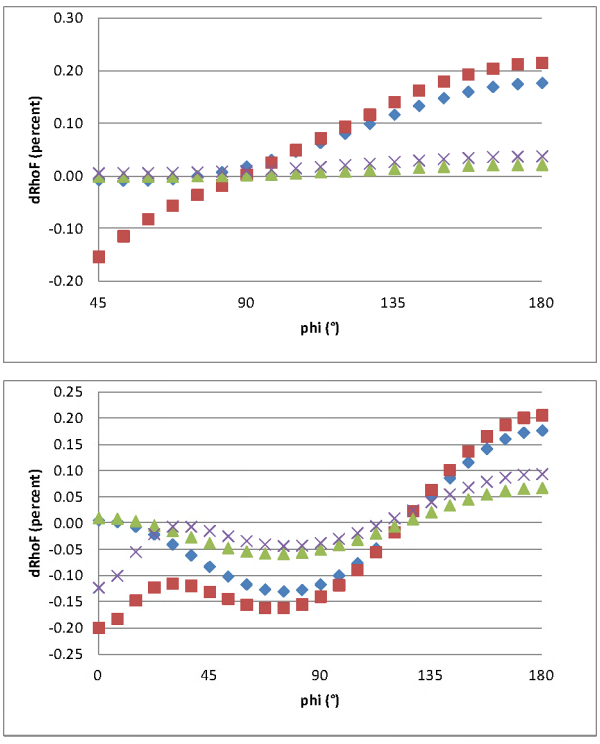

Figure 15: Same as figure 14 but with the aerosol model M4 with AOT560=0.3

4. CONCLUSION

The fundamental idea is that a computation of the total intensity requires using a vector radiative transfer code. The outputs do not need experimental verifications because they are in line with Fundamental Optics. Having this, it is possible to correctly simulate first the atmospheric radiance and then it reflection by the surface. A synthetic data based was generated and described in a companion paper [4].

This study clearly stresses that the total intensity (radiance) measured above water is affected by the polarisation state of the sky light, at least when the *Fresnel* reflection of sea surface is highly polarized. In the blue region, the *Rayleigh* scattering is the major source of impact due to its high polarization. The effect is less important in the NIR region because the light scattering is reduced. Although the aerosols with a small size may be highly polarised, their impact remains noticeable in the same time at the larger wavelengths. A simple recommendation to reduce the impact of the polarisation is to take measurements at small VZA.

When the aerosols play an important role in the polarization processes, we need first to well know their state of polarization. The knowledge of the aerosol polarization relies on the *Mie*'s computations, using as inputs the micro-physical properties of these particles. For the aerosols with a small size, we trend towards the *Rayleigh-Gauss* regime with $(m\text{-}1)\ r/\lambda$ as a key parameter. The smaller the refractive index (m) is, the larger the polarization is. A sensitivity study driven by m suggests that an error on the knowledge of the aerosol polarization has a small impact on the sky dome correction. Nevertheless, it would be recommended to experimentally validate the aerosol polarization. Some of CIMEL instruments in AERONET are equipped with polarized filters and could be used to get those in-situ measurements.

At the end, the weakness of the standard protocol used to access the marine reflectance stresses the need to include the polarization in the correction of above water measurements for the sky dome reflection. Indeed, depending on the illumination geometry, the state of sea surface (level of roughness) and the atmosphere, the bias on the reflected sky radiance may induce several percents in relative errors on the marine reflectance deduced from in-situ measurements, when ignoring polarization.

In the framework of an ESA project, we address in a second companion paper [6] the correction of sky dome reflection for the SeaPRISM [7] and TriOS [1] measurements collected in the MERMAID data base [8]. In that case, the information we need to compute R are available in the MERIS L2 products: in the auxiliary data file with the barometric pressure and the wind speed, in the aerosol product with the AOT865 and α.

5 REFERENCES

1 Mobley, C.D., 1999. Estimation of the remote-sensing reflectance from above-surface measurements, *Applied Optics*, 38: 7442–7455.

2 Ruddick, K.G., V. De Cauwer, Y.-J. Park and G. Moore, 2006. Seaborne measurements of near-infrared water-leaving reflectance: The similarity spectrum for turbid waters, *Limnology & Oceanography*, 51(2): 1167–1179.

3 Deuzé, J.L., M. Herman, and R. Santer, 1989. Fourier series expansion of the transfer equation in the atmosphere-ocean system, *Journal of Quantitative Spectro-scopy & Radiative Transfer*, 41 (6): 483-494.

4 Zagolski, F., R. Santer and J.P. Huot, 2012 (this issue). POLREF: A New Simulator for Polarized Reflection Coefficients over Ocean.

5 Cox, C., and W. Munk, 1954. Measurements of roughness of the sea surface from photographs of Sun glitter, *Journal of Optical Society in America*, 44 (11): 838-888.

6 Barker, K., F. Zagolski, R. Santer, C. Kent, J.-P. Huot, K. Ruddick and G. Zibordi, 2012 (this issue). Sky Dome Correction For SeaPRISM and TriOS Above Water Radiometric Measurements in MERMAID.

7 Zibordi, G., B. Holben, I. Slutsker, D. Giles, D. D'Alimonte, F. Mélin, J.-F. Berthon, D. Vandemark, H. Feng, G. Schuster, B. Fabbri, S. Kaitala and J. Seppälä, 2009. AERONET-OC: a network for the validation of Ocean Color primary radiometric products. *Journal of Oceanic and Atmospheric Technology* 26: 1634-1651.

8 Barker, K., C. Mazeran, C. Lerebourg, M. Bouvet, D. Antoine, M. Ondrusek, G. Zibordi and S. Lavender, 2008. MERMAID: The MERis MAtchup In-situ Database. In 2nd MERIS (A)ATSR Users WorkshopFrascati, Italy. September 2008.

6) ACKNOWLEDGMENTS

This work was partially supported by the INTERREG 2 Seas program.through the ISECA project